

# Symmetric Strip Transmission Line Tee Junction\*

A. G. FRANCO†, MEMBER, IRE, AND A. A. OLINER‡, FELLOW, IRE

**Summary**—Several different network forms have been employed previously to characterize the symmetrical strip-line tee junction and the parameters of these networks have been obtained by various means. In this paper the available theoretical and experimental results are systematically correlated. A choice, based on design convenience, is made of the most appropriate network form, and recommendations are given for the values of each of the parameters in this representation. In some ranges, the available data were inadequate, and additional experimental results were taken in order to clarify the recommendations.

## I. INTRODUCTION

THE SYMMETRIC tee junction (shown in Fig. 1) is incorporated in a wide variety of strip transmission line microwave circuits. In order to realize accurate electrical design of these strip line components, it is necessary to have precise knowledge of the parameters which represent the tee. The characterization of the tee by a direct junction is inadequate, as it ignores the reactive effects associated with the power stored in the neighborhood of the junction.

Several different network forms may be employed to characterize the tee and are presented in the literature.<sup>1-3</sup> The "Waveguide Handbook,"<sup>1</sup> (hereafter referred to as WGH) contains results for an *E*-plane (series) tee in rectangular waveguide; these results may be adapted via a Babinet equivalence procedure to the case of the strip-line tee, as is discussed later. Included in the WGH presentation are an especially simple equivalent circuit, reproduced here in Fig. 2, and graphical information concerning the values of the elements in such a circuit. The equivalent circuit dual to that in Fig. 2 which applies to the strip-line tee is shown in Fig. 3 and is discussed further below. In the work performed at MRI<sup>2</sup> (Microwave Research Institute, Polytechnic Institute of Brooklyn), theoretical expressions for the elements of one of the equivalent circuits of the strip-line tee are derived and a comparison is made with experimental data taken at a single frequency. More extensive experiments were performed at SRI<sup>3</sup> (Stanford

Research Institute) and the results are presented in terms of an alternate equivalent circuit. There has never been a concerted effort, however, to correlate the various theoretical and experimental results for the purpose of drawing some conclusions as to the accuracy and usefulness of the available information. The approach of this paper is to first make a choice, based upon design convenience, of the most appropriate network form for the strip-line tee junction. Equivalence relations are then derived between the elements of this form and those of several other networks employed. The theoretical and experimental values are then translated via these equivalence relations and the results are critically compared. Where the discrepancies between the various approaches are large and the choice based on theoretical considerations is uncertain, additional measurements were taken at IBM.

Detailed comparisons are presented graphically in a form which closely follows that used in the WGH. Based on these comparisons, final recommendations are made.

## II. PRESENTLY AVAILABLE DATA

The WGH contains a set of design equations for the *E*-plane tee junction in rectangular waveguide in addition to the graphical presentation. The equations are stated to be either asymptotic relations or expressions valid in the static limit. Whereas the graphs are stated to be accurate to within a few per cent over most of the wavelength range, the equations presented are only simplified approximations to the expressions from which the numerical values given in the graphs were determined, and are, therefore, less reliable. For this reason, only the WGH graphical results are included in this paper.

The MRI theoretical expressions were obtained by the Babinet equivalence procedure from corresponding expressions for the *E*-plane tee junction in rectangular waveguide. In contrast to the WGH results, these expressions were derived by variational calculations and are valid at centerline reference planes.<sup>4</sup> The physical tee structure, the equivalent circuit for centerline representation of the tee, and the location of the terminal planes *T* and *T*<sub>3</sub> of this equivalent circuit are shown in Fig. 4. MRI theoretical and experimental results are presented in a context to be discussed later in Figs. 6 through 11. The equations used to obtain these theoretical results are discussed in Section III.

\* Received by the PGM TT, September 29, 1961; revised manuscript received, November 2, 1961.

† Thomas J. Watson Research Center, IBM Corporation, Yorktown Heights, N. Y.

‡ Microwave Research Institute, Polytechnic Institute of Brooklyn, N. Y.

<sup>1</sup> N. Marcuvitz, "The Waveguide Handbook," McGraw-Hill Book Co., New York, N. Y., pp. 336-339, 344-347; 1951.

<sup>2</sup> H. M. Altschuler and A. A. Oliner, "Discontinuities in the center conductor of symmetric strip transmission line," IRE TRANS. ON MICROWAVE THEORY AND TECHNIQUES, vol. MTT-8, pp. 328-339; May, 1960.

<sup>3</sup> S. B. Cohn, *et al.*, "Design Criteria for Microwave Filters and Coupling Structures," Stanford Research Inst., Menlo Park, Calif., SRI Project 2326, Tech. Rept. 3; pp. 23-29; August, 1958.

<sup>4</sup> A. A. Oliner, "Equivalent Circuits for Slots in Rectangular Waveguide," Microwave Res. Inst., Polytechnic Inst. of Brooklyn, N. Y., Rept. R-234, pp. 122-125; August, 1951.

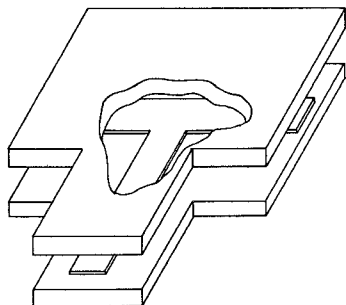


Fig. 1—Symmetric tee junction in symmetric strip transmission line.

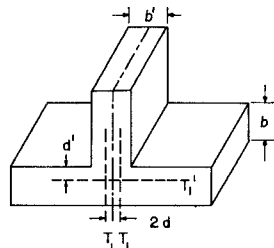


Fig. 2—Physical structure and equivalent circuit for *E*-plane tee junction in rectangular waveguide.

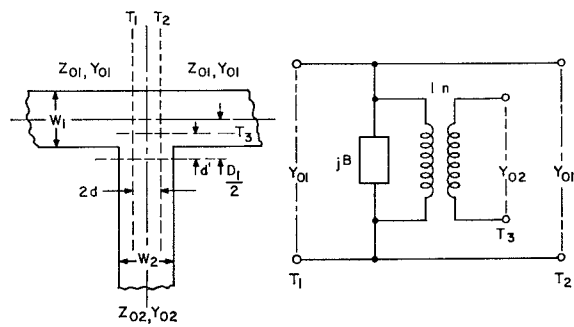


Fig. 3—Recommended equivalent circuit for strip-line tee junction.

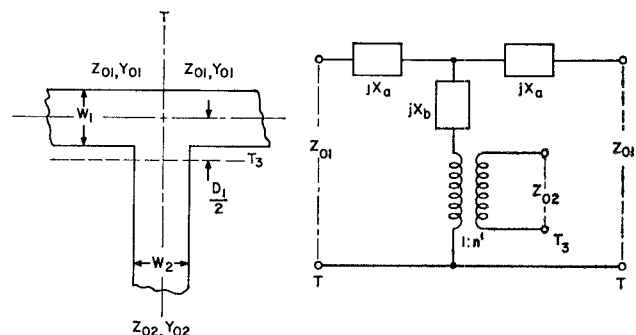


Fig. 4—MRI equivalent circuit for strip-line tee junction.

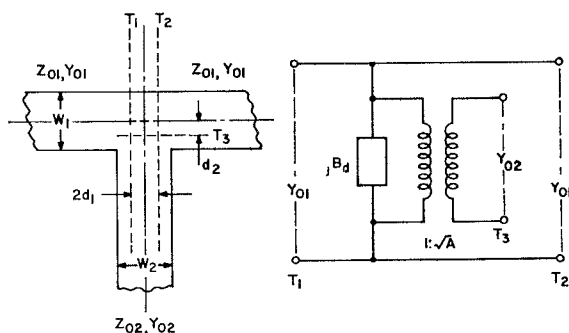


Fig. 5—SRI equivalent circuit for strip-line tee junction.

The network chosen by SRI to represent the tee junction is shown in Fig. 5. Comparison with Fig. 3 reveals the two circuits to be nearly identical. The SRI report presents, among other things, the measured equivalent circuit parameters for sixteen different symmetrical strip-line tee junctions. The experimental data is contained in appropriate context in Figs. 6 through 11.

### III. DISCUSSION OF AVAILABLE DATA

It is appropriate at this point to detail the method by which data obtained on an *E*-plane tee in rectangular waveguide can be employed to determine the parameters of a strip-line tee. The WGH results apply equally well to a parallel plate *E*-plane tee if  $\lambda$ , the wavelength of the TEM mode in parallel plate line, is substituted for  $\lambda g$ , the guide wavelength of the  $TE_{10}$  mode in rectangular

waveguide. The parallel plate structure may be modified without disturbing the fields by truncating the width and inserting magnetic sidewalls. By employing the Babinet equivalence procedure, wherein all magnetic walls are replaced by electric walls and vice versa, and all lines of *E* and *H* are replaced by lines of *H* and  $-E$ , respectively, an *H* plane (shunt) tee structure is derived. The dual of Fig. 2 now represents the equivalent circuit of this derived structure and the graphs of Figs. 6 through 11 (curves labeled WGH theory) may be applied to determine the elements of this circuit after the appropriate duality replacements are made.<sup>5</sup>

<sup>5</sup> For a more detailed explanation see A. A. Oliner, "Theoretical developments in symmetrical strip transmission line," *Proc. of Symp. on Modern Advances in Microwave Techniques*, Polytechnic Inst. of Brooklyn, N. Y., pp. 393-399; November, 1954.

The transformation from a parallel plate line of width  $D$  to a strip transmission line of strip width  $w$  and small strip thickness  $t$  is then given to a good approximation by<sup>2</sup>

$$D = w + \frac{2b \ln 2}{\pi} + \frac{t}{\pi} \left[ 1 - \ln \frac{2t}{b} \right], \quad (1a)$$

where  $b$  is the spacing between ground planes. For high-impedance lines, with  $w/b < 0.5$ , the more accurate relation<sup>2</sup>

$$D = bK(k)K(k') + \frac{t}{\pi} \left[ 1 - \ln \left( \frac{2t}{b} \right) \right] \quad (1b)$$

should be used, where  $K$  represents the complete elliptic integral of the first kind, and where the moduli  $k$  and  $k'$  are defined by

$$k = \tanh \left( \pi \frac{w}{2b} \right), \quad k' = (1 - k^2)^{1/2}.$$

The center strip of such a strip-line tee and the equivalent circuit obtained by taking the dual of Fig. 2 are indicated in Fig. 3. By the use of the transformations, the curves labeled WGH theory are derived from the curves on pages 344-347 of the WGH by replacing  $b/\lambda_g$  by  $2D_1/\lambda$ ,  $X/Z_0$  by  $B/Y_0$ , and  $b'/b$  by  $D_2/D_1$  or  $Z_{01}/Z_{02}$ .

A potentially dangerous error of typographical nature is also present in the WGH discussion. An inconsistency appears between the value of guide height  $b$  as employed in the graphs and in Fig. 6.1-1 of the WGH. As presented, some of the curves correspond to the situation for which the next higher mode can propagate in the main guide of the tee junction.<sup>6</sup> This inconsistency is cleared up most easily by maintaining Fig. 6.1-1 as is, and changing the parameter designation for the curves from  $b/\lambda_g$  to  $2b/\lambda_g$ .

A comment on the MRI results is necessary because of the differences between the presentations here and in the article by Altschuler and Oliner.<sup>2</sup> Fig. 4 differs from Fig. 22(b) of the above article<sup>2</sup> in that the characteristic impedances of the lines are specified directly here and are not normalized to unity. Consequently, the transformer turns ratio is given by  $n'$  rather than  $n$ , where

$$n = n' \sqrt{Z_{01}/Z_{02}} \quad \text{and} \quad n' = \frac{\sin(\pi D_2/\lambda)}{\pi D_2/\lambda}. \quad (2)$$

Also, parameters  $X_a'$  and  $X_b'$  are replaced by  $X_a$  and  $X_b$  where

$$X_a' = \frac{X_a}{Z_{01}}, \quad X_b' = \frac{X_b}{Z_{02}}.$$

<sup>6</sup> The authors are grateful to Dr. S. B. Cohn for bringing this point to their attention.

The expression relating  $X_a'$  to the strip-line tee geometry is

$$X_a' = -\frac{D_2}{\lambda} [0.785n]^2. \quad (3)$$

A similar, although more complicated, expression for  $X_b'$  is given by Altschuler and Oliner<sup>2</sup> but it is not reproduced here because parameter  $X_b'$  is not included in the recommendations made below, and will, therefore, not be needed. Further comments on the MRI results appear in Sections IV and V.

#### IV. RECOMMENDED CHOICE OF NETWORK FORM

As stated above, both the SRI circuit and the dual of the WGH circuit are nearly identical, the only difference appearing in notation. Because of its simplicity and the ease with which it can be combined with other networks, this is the recommended circuit configuration. Table I is a list of the notational changes necessary to make the SRI parameters conform to those of the recommended circuit of Fig. 3.

The MRI theoretical expressions obtained for the centerline representation of the tee may be transformed via appropriate lengths of transmission line so as to facilitate comparison with the WGH and SRI networks. This has been done and the comparisons are listed in Table II. Expressions relating  $n'$  and  $X_a/Z_{01}$  to the

TABLE I  
CORRELATION OF NOTATION BETWEEN THE PARAMETERS OF THE SRI AND THE RECOMMENDED EQUIVALENT CIRCUIT

SRI	Recommended
$A$	$n^2$
$d_2$	$\frac{D_1}{2} - d'$
$d_1$	$d$
$B_d$	$B$

TABLE II  
PARAMETERS OF THE RECOMMENDED EQUIVALENT CIRCUIT IN TERMS OF THOSE OF THE MRI EQUIVALENT CIRCUIT

1)	$n^2 = n'^2 \frac{\cos^2 \left( \frac{2\pi}{\lambda} d' \right)}{\cos^2 \left( \frac{2\pi}{\lambda} d \right)}$
2)	$\frac{B}{Y_{01}} + n^2 \frac{Y_{02}}{Y_{01}} \tan \left( \frac{2\pi}{\lambda} d' \right) = 2 \tan \left( \frac{2\pi}{\lambda} d \right)$
3)	$\tan \left( \frac{2\pi}{\lambda} d' \right) = \frac{Z_{01}}{Z_{02}} n'^2 \frac{X_b}{Z_{01}}$
4)	$\tan \left( \frac{2\pi}{\lambda} d \right) = -\frac{X_a}{Z_{01}}$

geometry of the tee junction have been given above as (2) and (3). In general, the representation of a symmetric lossless three-port requires four independent network parameters. The circuit of Fig. 4, however, contains only three independent elements. For completeness, it is necessary to include a transmission line of length  $l'$  in series with the transformer in the stub arm. Approximate theory predicts and experimental evidence<sup>2</sup> supports the contention that  $l'$  is very nearly zero. Its neglect became a source of concern, however, in developing the equations relating the MRI parameters to the recommended ones. Expressions equivalent to those in Table II were derived taking  $l'$  into account. Upon examination, however, it was found that the influence of  $l'$  was indeed very small and could be neglected.

#### V. DETAILED EVALUATIONS OF THE PARAMETERS

It is important to understand the significance of the relations obtained in Table II. The two networks of Figs. 3 and 4 are entirely equivalent at their respective terminal planes if the values of the parameters  $n$ ,  $B$ ,  $d'$  and  $d$  of Fig. 3 can be expressed in terms of the parameters  $n'$ ,  $X_a$ , and  $X_b$  of Fig. 4 according to the functional relations of Table II. This transformation process makes it difficult to compare the MRI theory to the WGH theory since, in general, a discrepancy in one parameter will affect all other parameters. For example, an error in  $d'$ , the location of the reference plane in the stub arm, will affect both  $B$  and  $n$ . In the discussion below, critical comparisons are made between the available theoretical and measured data for each of the parameters of Fig. 3.

##### A. Parameter $d'$ —Reference Plane Shift in the Stub Arm

The available data for  $d'$ , the reference plane shift in the stub arm, is summarized in Fig. 6. It is seen that there is indeed a discrepancy between the available theoretical results. The MRI theory looks too bunched with respect to the WGH results. The MRI experimental data must be regarded as inclusive since it was taken for only one value of  $2D_1/\lambda$ . Nevertheless, for low values of  $Z_{01}/Z_{02}$ , these MRI experimental results correlate more closely with the WGH values than with the MRI theory. The SRI data, while more extensive, is not available in that critical area where the discrepancy is greatest, *i.e.*, for  $2D_1/\lambda > 0.65$ . For those experimental points available, however, (including some values for  $Z_{01}/Z_{02} > 1.6$  not depicted here) the results also correlate more closely with the WGH values.

Because of the lack of definitive information, some additional experimental points were taken at IBM. This IBM experimental data is limited to one value of impedance ratio,  $Z_{01}/Z_{02} = 1$ , but includes three different values of  $2D_1/\lambda$ . The IBM data is regarded as most reliable and definitely shows a spreading out of  $d'$  as a function of  $2D_1/\lambda$ ; this spreading indicates that the WGH theory is the more reliable for this parameter.

Note also that the measured values of  $d'/D_1$  obtained at SRI and MRI for  $Z_{01}/Z_{02} = 1$  fall in line with the IBM experimental points. The bunching in the MRI theory is presumed to be due to unreliability in the theoretical expression for  $X_b/Z_{01}$  except for values of  $0.4 > 2D_1/\lambda > 0.6$ . The discrepancy in the value of  $n$  for  $2D_1/\lambda = 0.8$  supports the latter half of this claim. More will be said of this presently.

##### B. Parameter $n$ —Transformer Turns Ratio

In the Altschuler and Oliner paper,<sup>2</sup> there are two expressions given for  $X_b'$ ; the first valid in the region  $Z_{01}/Z_{02} < 0.5$ , the second for  $0.5 \leq Z_{01}/Z_{02} \leq 1.0$ . These values for  $X_b'$  were employed via equivalence relations 1) and 3) of Table II to determine  $n$ , the transformer turns ratio. In comparing these results with the WGH values for  $n$ , it was observed that significantly better agreement could be obtained if the region of validity for the second expression for  $X_b'$  were extended down to  $Z_{01}/Z_{02} = 0.2$ . This was done in plotting the curves labeled MRI theory in Fig. 7, where the other available data for  $n$  is also included.

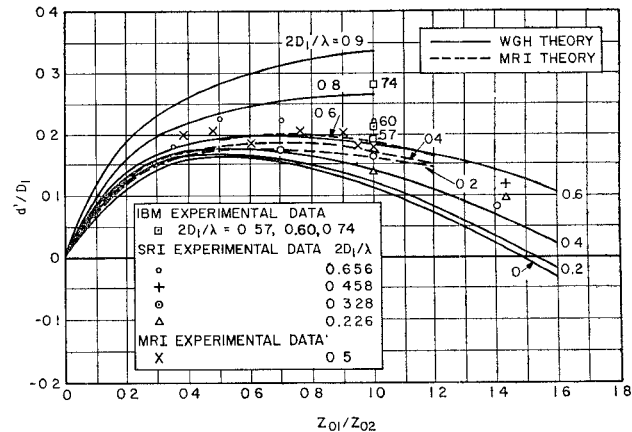


Fig. 6—Comparison among various theoretical and experimental results for parameter  $d'$ , the reference plane shift in the stub arm.

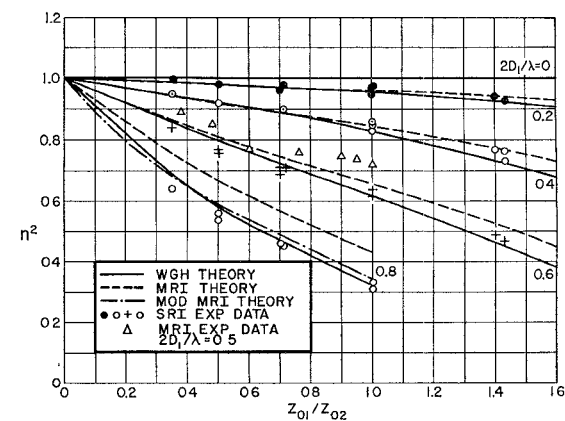


Fig. 7—Comparison among various theoretical and experimental results for parameter  $n$ , the transformer turns ratio.

Perhaps the first thing to be pointed out in examining Fig. 7 is the excellent agreement between the WGH theory and both the SRI and MRI experimental results. Agreement with MRI theory is also good except for  $2D_1/\lambda > 0.6$ , where the disparity is evident. Suppose now that the value of  $d'$  used in equivalence relation 1) of Table II is taken from the WGH theory and labeled  $d'_{WGH}$ , rather than from relation 3) of Table II which utilizes the values of  $X_a'$ . When  $n$  is computed using  $d'_{WGH}$ , the curves for  $2D_1/\lambda \leq 0.6$  are barely affected whereas for  $2D_1/\lambda = 0.8$  the curve is shifted down to the dot-dash line labeled "Modified MRI Theory" in Fig. 7. This modification results in excellent agreement among the various methods of determining  $n$ , and is stated as a revised equivalence relation in Table III. Further comments concerning Table III are made below; it may be noted however, that a relation corresponding to 3) is omitted since we recommend that  $d'$  be obtained from the WGH rather than from this relation.

TABLE III

MODIFIED PARAMETERS OF THE RECOMMENDED EQUIVALENT CIRCUIT IN TERMS OF THOSE OF THE MRI EQUIVALENT CIRCUIT

1a)	$n^2 = n'^2 \frac{\cos^2 \left( \frac{2\pi}{\lambda} [d'_{WGH}] \right)}{\cos^2 \left( \frac{2\pi}{\lambda} d \right)}$
2a)	$\frac{B}{Y_{01}} = 2 \tan \left( \frac{2\pi}{\lambda} d \right) - n^2 \frac{Y_{02}}{Y_{01}} \tan \left( \frac{2\pi}{\lambda} [d'_{WGH}] \right)$
4a)	$\tan \left( \frac{2\pi}{\lambda} d \right) = -0.7 \frac{X_a}{Z_{01}}$

### C. Parameter $d$ —Reference Plane Shift in the Main Arm

A third parameter in the recommended equivalent network is  $d$ , which locates the reference plane in the main arm. Because the shift  $d$  is relatively small and fairly difficult to measure accurately, previous efforts to characterize the tee have not yielded sufficiently accurate information concerning its value. The scatter in the SRI experimental points is so great that it was felt that the data could not possibly be meaningful. Correlation between the MRI and WGH theories is also extremely poor. Indeed, the only fortunate circumstance in determining the value of this parameter is that, due to the simple nature of the equivalence relation between  $X_a'$  and  $d$ , the two theories can be compared without regard to discrepancies in any of the other parameters.

In Fig. 8 the WGH theory is plotted alongside a curve labeled "Modified MRI Theory." The modification is simply the inclusion of a factor of 0.7 in the expression relating  $X_a'$  and  $d$  (see equivalence relation 4a) in Table III). The introduction of this factor is based on the following considerations: The numerical value for the reactance associated with  $X_a'$  is directly proportional

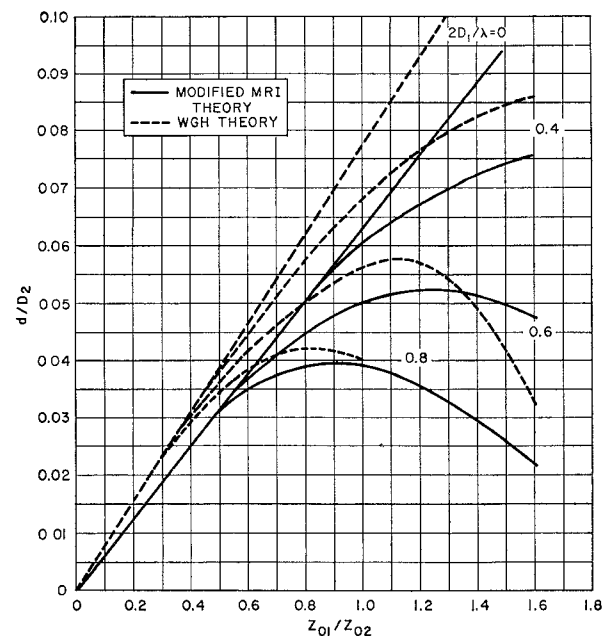


Fig. 8—Comparison of theories for parameter  $d$ , the reference plane shift in the main arms.

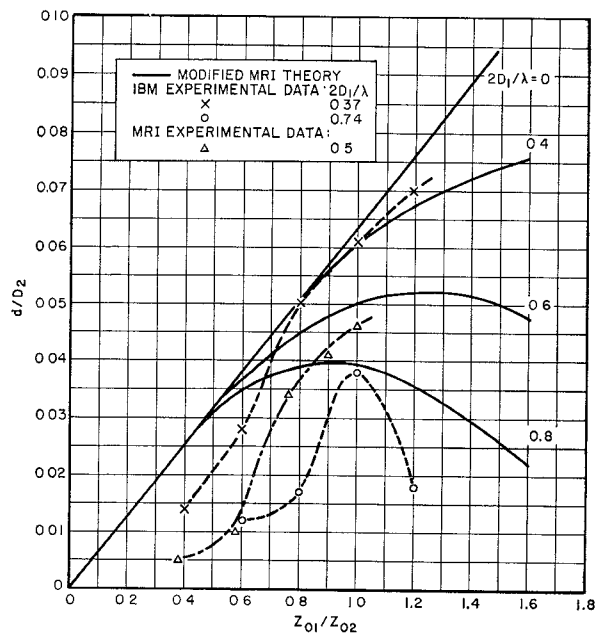


Fig. 9—Comparison between available experimental data and theory for parameter  $d$ , the reference plane shift in the main arms.

to the stored power (or equivalently, the distortion of the field lines) in the vicinity of the junction. By inspection, it is seen that more of this stored power appears in the main line than in the stub line. However, the unmodified expression given by Altschuler and Oliner<sup>2</sup> for  $X_a/Z_{01}$  assumes that the stored power in the stub line is the same as that in the main line. Hence this expression yields too large a reactance value. The optimal choice of 0.7 as a factor is based upon prior experience with meas-

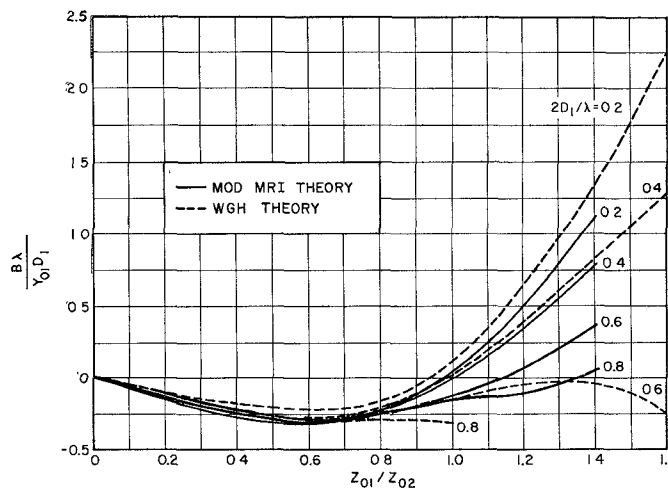


Fig. 10—Comparison of theories for parameter  $B$ , the susceptance element.

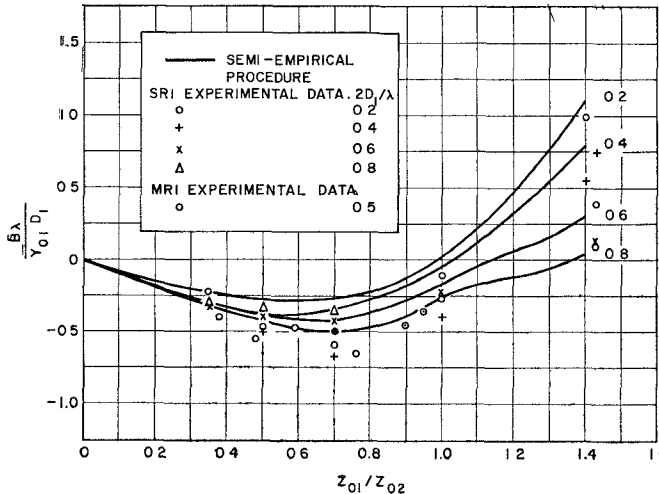


Fig. 11—Comparison between available experimental data and a semi-empirical procedure for  $B$ , the susceptance element.

urements on rectangular waveguide tee junctions.<sup>7</sup>

The above-described "Modified MRI Theory" was found to agree more closely with the available measured data than the WGH theory for parameter  $d$ . These theoretical values are given in Fig. 9, together with MRI and IBM measured data, the latter taken because of the dearth of otherwise available experimental information. The MRI and IBM data lend support to the 0.7 factor discussed above although the theory does not explain the behavior of this parameter over the whole range of  $Z_{01}/Z_{02}$  and  $2D_1/\lambda$ . For example, the behavior near the origin predicted by theory is linear whereas experimental results indicate a quadratic behavior. Also, for  $2D_1/\lambda=0.8$  the data indicates a more pronounced hump than does the theory. Note, however, that where theory and measured data differ significantly, the "Modified MRI Theory" provides a helpful

<sup>7</sup> A. A. Oliner, "Equivalent circuits for slots in rectangular waveguide," *Proc. of Symp. on Modern Advances in Microwave Techniques*, Polytechnic Inst. of Brooklyn, N. Y., pp. 225-227, November, 1954.

upper bound in locating the reference plane. Fig. 8 indicates that the WGH theory predicts even higher values of  $d$  almost everywhere and hence is not recommended.

#### D. Parameter $B$ —Shunt Susceptance

The remaining parameter to be discussed is the shunt susceptance  $B$ . A comparison between the WGH theory and the "Modified MRI Theory" is presented in Fig. 10. As seen from relation 2a) of Table III, the transformation from the MRI equivalent circuit to the recommended circuit causes  $B$  to be a function of  $n$ ,  $d'$  and  $d$ . It is not expected, therefore, that the MRI predicted values will be accurate in a region where the value predicted for either  $n$  or  $d$  is inaccurate. One such region occurs for all values of  $2D_1/\lambda$  and  $Z_{01}/Z_{02} < 1.0$ . Here  $d$  as predicted by the "Modified MRI Theory" is high, so that the use of these values of  $d$  would yield a  $B$  with too small a negative value. Comparison with the SRI and MRI measured data given in Fig. 11 substantiates this. Outside of this region, *i.e.*, for  $Z_{01}/Z_{02} \geq 1.0$ , better correlation is to be expected. The WGH theory plotted in Fig. 10 also yields a  $B$  with too small a negative value for  $Z_{01}/Z_{02} < 1.0$  and  $2D_1/\lambda < 0.6$ . In addition, it indicates a much larger sensitivity in this parameter with respect to  $2D_1/\lambda$  than is indicated by the measured data of Fig. 11. An alternative set of "theoretical" curves can be obtained on a semi-empirical basis by combining the "Modified MRI Theory" with values of  $d$  for  $Z_{01}/Z_{02} < 1.0$  and all values of  $2D_1/\lambda$ , which are experimental and are obtained from Fig. 9. This "Semi-Empirical Procedure" is plotted in Fig. 11 together with the SRI and MRI experimental values. It is seen that reasonable agreement is obtained by this procedure, and that the agreement is better than that found by using the curves of Fig. 10.

## VI. RECOMMENDATIONS

For the recommended network of Fig. 3 the following parameters must be determined:  $d'$ ,  $n$ ,  $d$ , and  $B$ .

#### A. Parameter $d'$ —Reference Plane Shift in Stub Arm

The recommended procedure for determining the value of this parameter can be stated very simply. Use WGH results for all ranges of  $Z_{01}/Z_{02}$  and all values of  $2D_1/\lambda$ . This conclusion is supported by both SRI and IBM measured data. The WGH results, which are presented here in Fig. 6, appear originally in Fig. 6.1-9 of the WGH, except that the quantities  $d'/b$  and  $b'/b$  should be replaced by  $d'/D_1$  and  $Z_{01}/Z_{02}$ . The parameter given there as  $b/\lambda_0$  becomes  $2D_1/\lambda$ . For values of  $2D_1/\lambda$  for which curves do not exist, one can either interpolate between curves or use (9) on page 338 of the WGH. The recommended procedure should enable the designer to be fairly accurate in his prediction for this parameter.

#### B. Parameter $n$ —Transformer Turns Ratio

To determine  $n$ , alternative recommendations are possible, depending on the predicted accuracy desired.

Use WGH results for values of  $2D_1/\lambda$  for which curves exist. These curves are given in Fig. 7 and in Fig. 6.1-10 of the WGH, where the appropriate changes in notation are the same as those indicated above for parameter  $d'$ . For all other values of  $2D_1/\lambda$  and for  $Z_{01}/Z_{02} \leq 1.0$ , one can alternatively interpolate between the curves or employ the MRI theoretical expressions, appropriately modified. This modification consists of computing  $n$  via equivalence relation 1a) of Table III, where  $n'$  is given by (2),  $d'_{WGH}$  has been discussed above,  $d$  is obtained from relation 4a) of Table III, and  $X_a/Z_0$  is given by (3). For  $Z_{01}/Z_{02} > 1.0$ , it is probably advisable to use WGH results as the MRI correction procedure was not checked in this range. Excellent agreement between the design and actual values should be obtained.

### C. Parameter $d$ —Reference Plane Shift in Main Arm

Here the recommendation to be made is a hybrid one. The IBM experimental data is considered the most reliable. The MRI experimental data appears to yield a value somewhat smaller than expected. For  $Z_{01}/Z_{02} < 1.0$  and for all values of  $2D_1/\lambda$ , interpolate between IBM curves (extrapolate curves if necessary). For  $Z_{01}/Z_{02} > 1.0$  and for all values of  $2D_1/\lambda$  use "Modified MRI Theory," which requires that  $d$  be computed from equivalence relation 4a) of Table III, where  $X_a/Z_0$  is given by (3). A fair prediction of the value of

this parameter should be obtained by utilizing the above procedure except possibly in the particular region where  $2D_1/\lambda > 0.7$  and  $Z_{01}/Z_{02} > 1.0$ . In this region only a helpful upper bound is available.

### D. Parameter $B$ —Shunt Susceptance

The curves obtained by the "Semi-Empirical Procedure" and plotted in Fig. 11 should be utilized to determine the value of the parameter  $B$ . This is also a hybrid recommendation as these curves were drawn by combining IBM experimental data for parameter  $d$ , for the range  $Z_{01}/Z_{02} < 1.0$  and for all values of  $2D_1/\lambda$ , with "Modified MRI Theory." The latter requires the computation of  $B$  via equivalence relation 2a) of Table III, where the parameters occurring in this relation have been discussed above. The curves are to be taken as fairly reliable except for  $2D_1/\lambda > 0.7$  and  $Z_{01}/Z_{02} > 1.0$ , where the experimental drop-off in  $d$  would indicate a lower value for  $B$ .

### ACKNOWLEDGMENT

The authors are indebted to George F. Bland of IBM for his initiation of this study, his many helpful suggestions, and his continued interest and encouragement. They are also grateful to William R. Jones, formerly of IBM, who contributed substantially to this effort in its initial stages.

## The Use of Exponential Transmission Lines in Microwave Components\*

CHARLES P. WOMACK†, MEMBER, IRE

**Summary**—This paper describes some techniques for utilizing exponential transmission lines in microwave components in order to reduce element lengths, and hence size and weight, and to significantly increase the operating frequency range. Formulas are developed which relate line length to the frequency and rate of taper for transmission line resonators, and a nomogram is included for easy determination of spurious frequencies. Additional formulas are given for the distributed representation of lumped elements using exponential sections of both coaxial and strip transmission line, and their use described in application to microwave filters and related components. In addition, the paper describes how unusually large rejection bandwidths can easily be obtained by proper selection of the individual element lengths and rates of taper.

\* Received by the PGMTT, July 31, 1961; revised manuscript received, November 6, 1961. The work reported in this paper was supported in part by the Wilcox Electric Co., Inc., Kansas City, Mo., under Contract No. CRES-17 to the Center for Research in Engrg. Science, University of Kansas, Lawrence, Kan.

† Collins Radio Company, Cedar Rapids, Iowa. Formerly with the University of Kansas, Lawrence, Kan.

### INTRODUCTION

IN THE LAST few years there has been a growing awareness of the need for new designs of microwave components which combine the advantages of decreased size and weight, ease of fabrication, and extended coverage of the microwave spectrum. In this paper various techniques for designing microwave components using exponential transmission line sections will be presented and their advantages and limitations will be considered. In particular it will be shown that the use of exponential sections of strip transmission line in the design of microwave filters offers significant savings in volume and weight, variable form factors, greatly extended rejection bandwidths, and the same ease of construction as with other strip-line components. Formulas are developed which relate line length to the fre-